NeuroImage 244 (2021) 118581

Contents lists available at ScienceDirect

NeuroImage

journal homepage: www.elsevier.com/locate/neuroimage

Multisensory integration in cortical regions responding to locomotion-related visual and somatomotor signals

Sara Di Marco[a,b,1,*], Valentina Sulpizio[a,b,1], Martina Bellagamba[b,c], Patrizia Fattori[d], Gaspare Galati[a,b], Claudio Galletti[d], Markus Lappe[e,f], Teresa Maltempo[b,c], Sabrina Pitzalis[b,c]

[a] Department of Psychology, "Sapienza" University of Rome, Rome, Italy
[b] Department of Cognitive and Motor Rehabilitation and Neuroimaging, Santa Lucia Foundation (IRCCS Fondazione Santa Lucia), Rome, Italy
[c] Department of Movement, Human and Health Sciences, University of Rome "Foro Italico", Rome, Italy
[d] Department of Biomedical and Neuromotor Sciences, University of Bologna, Bologna, Italy
[e] Institute for Psychology, University of Muenster, Muenster, Germany
[f] Otto Creutzfeldt Center for Cognitive and Behavioral Neuroscience, University of Muenster, Muenster, Germany

ARTICLE INFO

Keywords:
Egomotion
Optic flow
Heading changes
Leg movements
Footstep
fMR-adaptation paradigm

ABSTRACT

During real-world locomotion, in order to be able to move along a path or avoid an obstacle, continuous changes in self-motion direction (*i.e.* heading) are needed. Control of heading changes during locomotion requires the integration of multiple signals (*i.e.*, visual, somatomotor, vestibular). Recent fMRI studies have shown that both somatomotor areas (human PEc [hPEc], human PE [hPE], primary somatosensory cortex [S-I]) and egomotion visual regions (cingulate sulcus visual area [CSv], posterior cingulate area [pCi], posterior insular cortex [PIC]) respond to either leg movements and egomotion-compatible visual stimulations, suggesting a role in the analysis of both visual attributes of egomotion and somatomotor signals with the aim of guiding locomotion. However, whether these regions are able to integrate egomotion-related visual signals with somatomotor inputs coming from leg movements during heading changes remains an open question. Here we used a combined approach of individual functional localizers and task-evoked activity by fMRI. In thirty subjects we first localized three egomotion areas (CSv, pCi, PIC) and three somatomotor regions (S-I, hPE, hPEc). Then, we tested their responses in a multisensory integration experiment combining visual and somatomotor signals relevant to locomotion in congruent or incongruent trials. We used an fMR-adaptation paradigm to explore the sensitivity to the repeated presentation of these bimodal stimuli in the six regions of interest. Results revealed that hPE, S-I and CSv showed an adaptation effect regardless of congruency, while PIC, pCi and hPEc showed sensitivity to congruency. PIC exhibited a preference for congruent trials compared to incongruent trials. Areas pCi and hPEc exhibited an adaptation effect only for congruent and incongruent trials, respectively. PIC, pCi and hPEc sensitivity to the congruency relationship between visual (locomotion-compatible) cues and (leg-related) somatomotor inputs suggests that these regions are involved in multisensory integration processes, likely in order to guide/adjust leg movements during heading changes.

1. Introduction

Egomotion (or self-motion) perception relies on the integration of sensory information arising from different modalities, including visual, vestibular, somatosensory and motor signals (for a review, see Greenlee et al. 2016). In turn, these integrated signals are recursively used for controlling egomotion itself. Continuous changes in heading direction (*i.e.*, direction of self-motion) are needed for spatial exploration and navigation through the surrounding environment. Optic flow generated on the retina as a visual feedback of self-motion provides important visual information, such as instantaneous heading and path curvature (Li and Cheng, 2011; Crowell and Banks, 1993; Cutting et al., 1997).

Abbreviations: CSv, cingulate sulcus visual area; hPE and hPEc, human PE and human PEc; MST, medial superior temporal area; PBA, parietal body area; macaque PE and PEc, P stands for Parietal, E stands for the specific parietal area 'E' based on the von Economo and Koskinas classification (1925), c stands for caudal; pCi, posterior cingulate area; PIC, posterior insular cortex; ROIs, regions of interest; S-I, primary somatosensory cortex; VIP, ventral intraparietal area; VPS, visual posterior sylvian area.

* Corresponding author at: Department of Psychology, "Sapienza" University of Rome, Via dei Marsi, 78, Rome 00185, Italy.
E-mail address: contact.saradimarco@gmail.com (S. Di Marco).

[1] These authors contributed equally to this work.

https://doi.org/10.1016/j.neuroimage.2021.118581.
Received 18 May 2021; Received in revised form 8 September 2021; Accepted 14 September 2021
Available online 17 September 2021.

During natural locomotion, there are also somatomotor signals which are sent from the lower limbs and are taken into account for guiding subsequent movements. Importantly, such visual and somatomotor sensory signals need to be merged with the aim of controlling self-motion during locomotion. Lower limb movements are likely planned according to the expected visual feedback. However, little is known about which cortical areas are responsible for such visuo-somatomotor integration.

In monkeys, area PEc is a somatomotor region located in the posterior parietal cortex which has been shown to contain unimodal somatosensory cells responding to passive joint manipulation of both arm and leg (Breveglieri et al., 2006; Gamberini et al., 2018) and unimodal visual cells responding to radial optic flow and the direction of heading in the visual field (Battaglia-Mayer et al., 2001; Raffi et al., 2002, 2010, 2011, 2014). Macaque PEc also hosts bimodal visual-somatosensory neurons responding to passive limb manipulation and complex visual stimuli rapidly changing in size and shape (Breveglieri et al., 2008; Gamberini et al., 2018). Based on this evidence, it has been suggested that PEc is able to integrate visual and somatomotor information for whole-body interaction with the visual environment, including locomotion (Breveglieri et al., 2008; Gamberini et al., 2018), even though bimodal visual-somatosensory cells have never been tested with optic flow stimuli. This is further supported by a study showing that macaque PEc is strongly connected with the dorsomedial portion of the somatomotor cortex, representing lower limbs, and the cingulate motor regions and vestibular areas (Bakola et al., 2010).

On the other hand, monkey multisensory regions known to be sensitive to visual motion, namely areas MST, VIP and VPS, are also implicated in multimodal estimate of heading by combining visual and vestibular cues to self-motion direction (Duffy, 1998; Bremmer et al., 1999; Schlack et al., 2002; Gu et al., 2006, 2008; Chen et al., 2011a, 2011b, 2013).

In humans, the homologue of macaque PEc (hPEc) has been recently identified based on its response to active movements of both arm and leg (Pitzalis et al., 2019). In line with macaque data, human PEc also shows visual sensitivity to egomotion-compatible coherent visual motion (*i.e.* flow fields stimulus, Pitzalis et al. 2019). Anterior to hPEc, positive BOLD responses to leg movements were detected also in areas hPE and S-I (Pitzalis et al., 2019). hPE likely corresponds to the leg representation of macaque area PE (Gamberini et al., 2020) and its anatomical position fits well with the medialmost portion of area PBA (Parietal Body Area; Huang et al., 2012), the multisensory parietal homunculus containing overlapping somatotopic and retinotopic maps (Huang et al., 2012). Consistent with human evidence about visual responses in the cortical territory occupied by hPE, this region (differently from S-I) shows a marginally significant response to the egomotion-compatible flow field stimulus (Pitzalis et al., 2019). Since in that paper we defined these areas by using a somatomotor task hereafter we refer to hPEc, hPE and S-I as three leg-related somatomotor regions.

Among the well-known egomotion-related visual regions, areas CSv, pCi, and PIC, but not V6+, V3A, and VIP, respond to both the flow field stimulus and active leg movements, suggesting a role in the control of visually-guided locomotion (Serra et al., 2019). In addition, in a very recent paper of our lab (Di Marco et al., 2021), we found that hPEc, hPE, S-I, CSv and pCi show a preference for an optic flow stimulus that simulates a locomotion-compatible curved path, suggesting that these regions are involved in encoding heading changes and in the estimation of path curvature. This is needed for recovering the future direction of self-motion and for controlling steering actions and locomotor stability during heading changes. CSv and pCi prefer forward visual motion (as compared to backward visual motion), suggesting their involvement in a fine visual analysis of the external world toward which one is moving during locomotion.

Taken together, these findings strengthen the idea that these multisensory regions are implicated in the analysis of both visual attributes of egomotion and somatomotor signals related to the legs with the likely aim of guiding locomotion (Pitzalis et al., 2019; Serra et al., 2019; Di Marco et al., 2021). Since cortical sensitivity to multisensory information does not necessarily entail multisensory integration of such information, here we are interested in verifying whether the above-mentioned cortical regions are able to integrate egomotion-like visual information with somatomotor signals from the lower limbs for the control of visually-guided locomotion during heading changes remains an open question.

To address this matter, we used a combined approach of individual surface-based analysis and task-evoked paradigms by fMRI aimed at revealing integration mechanisms in key cortical areas for locomotion control, providing simultaneously locomotion-relevant visual and somatomotor stimuli in congruent and incongruent combinations.

We mapped on the individual surface of each subject two sets of multisensory regions of interest (ROIs) using dedicated functional localizers. First, we defined three leg-related somatomotor regions (hPEc, hPE and S-I) by a modified version of the somatomotor task recently employed in Pitzalis et al. (2019), and three egomotion-related visual regions, which are known to respond also to leg movements (visuomotor areas; Serra et al. 2019), by using a visual motion task (Pitzalis et al., 2010). Afterwards, to find any multisensory integration evidence, we tested the response of all these independently defined ROIs in the main fMRI 'Visuo-Somatomotor Multisensory Integration' experiment. Subjects were asked to execute a leg movement simulating a footstep towards right or left while presented with a simultaneous optic flow stimulus simulating a changing heading towards right or left. In such a way we manipulated the spatial congruency between visual and somatomotor stimuli (*i.e.*, congruent and incongruent combinations) by which only bimodal neurons, which are responsible for multisensory integration, are affected (van Atteveldt et al., 2010). Hence, a region which is sensitive to such congruency relationship by showing a preference for congruent or incongruent combinations should be involved in multisensory integration. We opted for an fMR-adaptation paradigm (*i.e.*, showing a reduction of the neural response to repeated trials compared to non-repeated trials as evidence of sensitivity to the repeated feature) where a region implicated in multisensory integration might either adapt stronger for congruent as compared to incongruent pairs or show the opposite pattern. Finding such adaptation effect related to congruent/incongruent manipulation in a cortical region might suggest that the region is able to integrate multimodal sensory cues, possibly with the aim of guiding locomotion, a functional role that has been hypothesized based on sensitivity to both leg movements and radial optic flow tested separately (Pitzalis et al., 2019; Serra et al., 2019; Di Marco et al., 2021).

2. Materials and methods

2.1. Subjects

Thirty right-handed and right-footed healthy adults (mean age: 25, SD = 3, 18 males) participated in this study. The sample size was determined based on previous similar fMRI studies (Frank et al., 2014; Schindler and Bartels, 2018a, 2018b). All subjects completed in different days two functional magnetic resonance imaging (fMRI) sessions. In the first session they performed the main event-related fMRI Visuo-Somatomotor Integration experiment. In the second session they participated in two localizer scans to define three somatomotor areas (hPEc, hPE and S-I) and three egomotion regions (CSv, PIC and pCi), respectively. All subjects had normal or corrected-to-normal visual acuity and no history of psychiatric or neurological disease. Hand and foot right-dominance were tested by the Edinburgh handedness inventory (Oldfield, 1971). These inclusion criteria were established prior to data collection and analyses. All participants gave written informed consent and all procedures were approved by the Ethics Committee of Fondazione Santa Lucia, Rome, Italy.

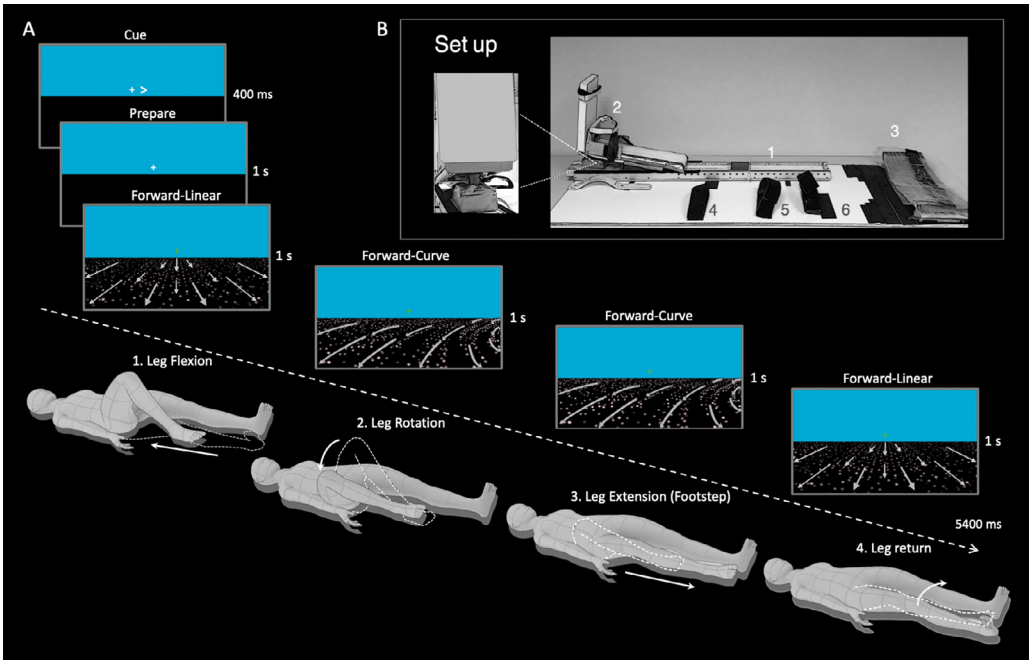

Fig. 1. Visuo-somatomotor integration experiment and set-up. (A) Representation of a congruent trial with both visual and somatomotor stimuli showing a changing heading toward right. 3D manikins indicate the sequence and kinematic of leg movements and the coupling with the visual stimulation, specifically: 1 s "leg flexion phase" matched with 1 s "forward-linear phase"; 1 s "rotation phase" and 1 s "extension phase" matched with 2 s "forward-curve phase"; 1 s "return phase" matched with 1 s "forward-linear phase". (B) The in-house MRI-compatible set-up for leg movements. On the left panel, a close-up of the cardan joint (see Methods for details).

2.2. Visuo-Somatomotor integration experiment

An event-related main fMRI experiment, hereafter called *Integration experiment*, was used to explore cortical sensitivity to multisensory integration of signals relevant for locomotion, such as visual motion cues and somatomotor signals coming from leg movements. For this purpose, two simultaneous conditions were employed: a visual-motion condition providing unimodal visual input and a pure somatomotor condition providing unimodal somatomotor input (see Fig. 1A). For sake of clarity, although in this study we used only bimodal conditions (*i.e.*, visual-motion and somatomotor conditions are always simultaneously presented), the two unimodal conditions are separately described below.

The visual motion condition consisted of passive viewing of a virtual 3D environment with blue sky filling the upper visual field and a black ground plane filling the lower visual field. The general layout of the visual stimulation is identical to that used in a recent paper from our lab (Di Marco et al., 2021). A white central fixation cross was placed slightly above the horizon. The black ground plane was filled with white dots moving in a coherent manner to simulate egomotion-compatible visual feedback. Dots were randomly generated online at each trial and their size and local speed were radially scaled with distance from the observer. Dots traveled at an average speed of 2°/s to give participants the impression they were simulating a footstep. In each trial, dots moved according with two phases: (1) a 1 s "forward-linear phase" simulating forward linear motion, (2) a 2 s "forward-curve phase" simulating forward curve motion toward right or left, so as to reproduce locomotion-compatible heading changing from linear path to rightward or leftward curve path. Finally, 1 s forward linear motion equal to the initial 1 s "forward-linear phase" was presented.

In the somatomotor condition subjects were asked to perform a long-range leg movement simulating a footstep toward right or left using the leg-set-up (Fig. 1B; see Experimental set-up for details). They initially maintained both legs laid down on the scanner bed. Each trial started with a visual cue signal appearing for 400 ms at the right or left side of the fixation cross to inform the subject on the direction in which the footstep had to be executed. After a 1 s interval for movement preparation, the fixation cross turned green (go signal) for 4 s and subjects started to execute a sequence of lower limb movements reproducing a footstep toward right or left as instructed. Specifically, the lower limb movement consisted of four phases: (1) a 1 s "flexion phase" of flexion of the right leg with gradual dorsi-flexion of the right foot, (2) a 1 s "rotation phase" of rightward or leftward rotation of the right leg, (3) a 1 s "extension phase" of extension of the right leg with gradual dorsi-extension of the right foot to simulate a complete footstep; (4) finally, 1 s return movement back to the starting position was performed.

Outside the scanner, subjects underwent an extensive training (lasting about 30 min) to execute the leg movement according to the required sequence and timing in order to perform it synchronized with changes in the visual motion stimulus. Fig. 1A shows the kinematic of the leg movements and the coupling with the visual motion stimulation. In particular, 1 s "leg flexion phase" matched with 1 s "forward-linear phase" corresponding to the phase when the foot lifts off the ground and the body moves forward on a linear path, while 1 s "rotation phase" and 1 s "extension phase" matched with 2 s "forward-curve phase" corresponding to the phase when the body rotates while keeping moving forward thus travelling on a curve path and the foot prepares for landing. Finally, 1 s "return phase" matched with 1 s "forward-linear phase" corresponding to the phase when the body keeps going forward on a linear path. Due to the scanner limitations, the leg movement speed was kept low to avoid excessive head and body motion. Thus, a low velocity was used for the visual motion stimulation in order to approximately match the visually-induced self-motion velocity with that of the leg movement. The preparation interval of constant length (1 s) after the cue signal ensured that the trained subjects started their leg movement at the go signal so that each phase of the leg movement matched with the corresponding phase of the visual motion stimulus. More importantly, the green fixation cross lasting 4 s gave participants visual feedback on the temporal window for executing the entire sequence of movements. Specifically, subjects were instructed to start performing the movement when the fixation cross turned green and to complete the sequence of movements coming back to the starting position when the cross turned white.

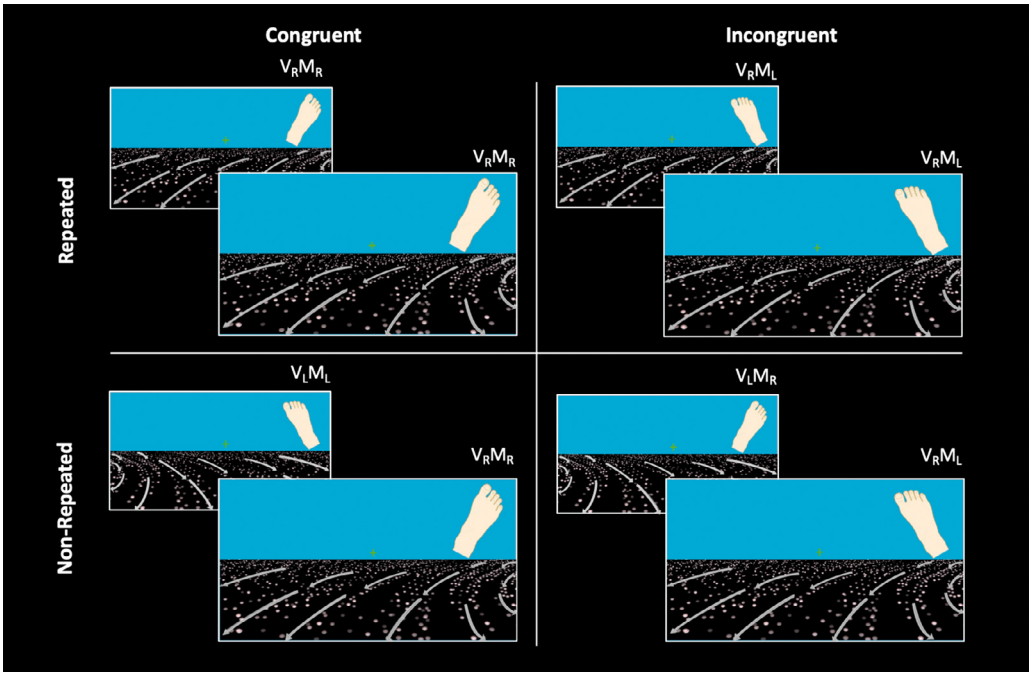

Fig. 2. 2 by 2 factorial design Congruency x Repetition: bimodal combinations of rightward or leftward visual and somatomotor unimodal stimuli (forward-curve visual motion and footstep) resulted in congruent and incongruent trials which were classified as repeated or non-repeated based on the previous trial accordingly with the fMR-adaptation paradigm. Bimodal combinations of right (R) or left (L) direction independently manipulated in the visual component, *i.e.*, simulating forward linear motion changing to forward curve motion toward right (V_R) or left (V_L) and in the somatomotor component, *i.e.*, a footstep executed toward right (M_R) or left (M_L), resulted in two congruent combinations (V_RM_R, V_LM_L) and two incongruent combinations (V_RM_L, V_LM_R).

Bimodal combinations of right (R) or left (L) direction independently manipulated in the visual component, *i.e.*, simulating forward linear motion changing to forward curve motion toward right (V_R) or left (V_L) and in the somatomotor component, *i.e.*, a footstep executed toward right (M_R) or left (M_L), resulted in two congruent combinations (V_RM_R, V_LM_L) and two incongruent combinations (V_RM_L, V_LM_R) (Fig. 2).

Subjects were instructed to fixate throughout the experiment the central cross informing about the timing of the somatomotor task. Additionally, the central cross simulated observer gaze direction so that fixation ensured that subjects received a visual stimulation that properly simulated their motion in both linear and curve phases. In other words, keeping central fixation, participants' gaze direction was aligned with the linear trajectory of dots flow during the linear phase and tangential to the direction of the curving trajectory of dots flow during the curve phase (for further details see Di Marco et al. 2021).

Accordingly with the fMR-adaptation paradigm, all the above-mentioned bimodal (congruent or incongruent) combinations were arranged so that each bimodal combination was classified as repeated or non-repeated based on the previous trial (see Fig. 2). This gave a 2 by 2 factorial design Congruency x Repetition resulting in four experimental conditions: (1) Repeated Congruent condition in which V_RM_R was preceded by V_RM_R, and V_LM_L was preceded by V_LM_L; (2) Non-Repeated Congruent condition in which V_RM_R was preceded by V_LM_L and vice versa; (3) Repeated Incongruent condition in which V_RM_L was preceded by V_RM_L and V_LM_R was preceded by V_LM_R; (4) Non-Repeated Incongruent condition in which V_RM_L was preceded by V_LM_R and vice versa.

Note that, since we were interested in studying multisensory integration processes by comparing congruent and incongruent combinations, only the bimodal stimulus per se was repeated, meaning that there were no trials in which only one unimodal component was repeated. This led to the following scenario: in the repeated condition, the direction of each unimodal component was identical to that of the previous trial, whereas in the non-repeated condition, the direction of each unimodal component was opposite to that of the previous trial. As a consequence, congruent and incongruent trials were separated in different blocks. Importantly, each unimodal stimulus was presented for the same number of times in congruent and incongruent blocks, in order to balance across congruent and incongruent conditions the adaptation of unimodal neurons for the repetition of the unimodal stimulus in their preferred sensory modality (*i.e.*, unimodal neurons adapt equally stronger in both congruent and incongruent conditions). This ensures that any difference in the adaptation effect between congruent and incongruent blocks can be ascribed only to bimodal neurons. Indeed, only bimodal neurons are sensitive to the congruency relationship between unimodal stimuli. Conversely, unimodal neurons are insensitive to such a congruency relationship, thus can only be responsible for an adaptation effect independent from congruency. Congruent and incongruent blocks were equally distributed throughout each run. Experimental blocks were randomly interleaved with 13.2 s fixation periods (rest), in which only the visual stimulus with no dots moving along the ground plane was presented. Fixation periods represented the baseline in this experiment. Each bimodal congruent and incongruent condition, categorized based on fMR-adaptation paradigm (repeated or non-repeated), was presented 12 times per run. Each subject completed 4 runs. This gave a total of 48 repetitions per condition.

To encourage good fixation, subjects were instructed to perform a blinking detection task at fixation. They were asked to detect a blink of the fixation cross, lasting 50 ms and occurring a variable number of times, from 4 to 6, in each run. At the end of each scan participants verbally reported the number of times in which the fixation cross blinked. Behavioral responses were recorded, and subjects received feedback on their ability to maintain a steady fixation. As for the somatomotor task, maintaining gaze on the central cross allowed participants to follow experiment instructions which were provided at fixation besides ensuring that no confounding signal associated with eye movements was added. The percentage of accuracy for the visual task averaged across subjects was 90% (SD = 9.75), indicating a good capability of the participants to maintain a constant attentional state throughout all the

visuo-somatomotor integration experiment. Experimenters were engaged throughout the experiment in the visual inspection of the task performance for each trial, verifying whether the correct sequence of movements was executed and checking the direction of the performed footstep (right or left) in order to assess accuracy in following cue instruction (right or left). Indeed, spatial congruency relationship between visual and somatomotor inputs in each trial strictly depended on the direction of the executed footstep. Again, the percentage of accuracy for the somatomotor task averaged across subjects was equal to 99% (SD = 1.36), indicating that participants in most of the trials correctly performed the footstep in the instructed direction. Note that the sequence of movements was always executed correctly, indicating that the pre-scanning training was effective.

2.3. Localizer scans

In a second set of fMRI experiments, several localizer scans were conducted to define three leg-related regions (hPEc, hPE and S-I) similar to the somatomotor task used in Pitzalis et al. (2019) and three egomotion regions (CSv, pCi and PIC) based on the visual motion task used in Serra et al. (2019). The specific procedures are described in detail below.

Localizer for hPEc, hPE and S-I ROIs (*leg movement scans*). Subjects were asked to perform a modified version of the somatomotor task used in Pitzalis et al. (2019) requiring to execute the same long-range leg movement simulating a footstep as the visuo-somatomotor integration experiment, in order to maximally stimulate limbs joints and activate somatomotor neurons (see above for a detailed description of the movement sequence). Each scan consisted of 4 consecutive trials for each block for a total of fourteen leg movement blocks lasting 20.5 s each, interleaved with 14 fixation periods of variable duration (12, 14 or 16 s). During fixation blocks, subjects were asked only to maintain fixation throughout the block. In experimental blocks, the white fixation cross turned red for 300 ms (warning signal for the movement preparation) and, after a variable delay (750, 1000, 1250, 1500 ms), turned green (go signal) for 4 s, instructing participants to execute a 4 s sequence of limb movement while keeping central fixation.

Localizer for CSv, pCi and PIC ROIs (*flow fields scans*). Briefly, participants were instructed to maintain central fixation while presented with four 16-s blocks of coherently moving dot fields interleaved with four 16-s blocks of randomly moving dot fields (flow fields stimulus). A new field of white dots was generated every 500 ms. During blocks of coherent motion, a new field of white dots was generated every 500 ms showing randomly a different motion pattern ranging from dilations, contractions, spirals and rotations. The center of the movement was jittered from flow to flow, and the dot speed was logarithmically scaled with eccentricity (average speed: 25°/s; range of speed variance: 17°/s – 33°/s; see Pitzalis et al., 2010 for a detailed description).

2.4. Experimental set-up

In both the Integration experiment and the localizer for the three leg-related somatomotor regions, we used an in-house MRI-compatible set-up allowing subjects to perform controlled and fluid leg movements. This leg-movement set-up was recently developed by our group and it is described in detail elsewhere (*e.g.*, Serra et al. 2019 , Pitzalis et al. 2019). Briefly, it consisted of an aluminum track fixed via Velcro straps on a wooden table which perfectly fitted the scanner bed (Fig. 1B). Subjects laid down on the wooden table, with their right leg extended along an aluminum-track (1) and with their right foot comfortably fixed with elastic straps to an aluminum support (2) which sliding along the track allowed subjects to perform fluid and controlled long-range leg flexion and extension. Velcro straps for immobilizing hip (3), tight (4), knee (5) ankle (6) of the left leg controlled for whole-body movements. Importantly, for the present study a cardan joint (close-up in Fig. 1B) was added to the aluminum foot support, allowing movement adjustments in each direction in order to ensure wide and smooth rotations of every right leg joint both rightward and leftward and free and smooth ankle flexions and extensions during the footstep execution. Smooth leg and ankle movements were important for providing somatomotor input that was as natural as possible during both the integration experiment and the leg movement scans. This methodological refinement represents a crucial difference with respect to what done in the past. Indeed, likely due to technical limits preventing the use of complete long-range movements in the MR environment, the few previous studies focusing on lower limbs used simple leg or foot movements mainly including ankle rotation (Heed et al., 2011, 2016; Leoné et al., 2014; Sood and Sereno, 2016) or ankle dorsiflexion (Sahyoun et al., 2004; Christensen et al., 2007; Kapreli et al., 2008; Rocca and Filippi, 2010; Lorey et al., 2014; Dalla Volta et al., 2015; Sacheli et al., 2017), but neglecting the hip joint, which has a fundamental role in guiding locomotion. A second training was shortly performed also in the scanner with subject's leg secured to the set-up for executing leg movements as smooth and naturally as possible without moving head and other body parts. After training, participants were able to automatically execute the entire sequence of lower limb movements in a smooth way as if they were actually performing a footstep. Notably, the possible degrees of freedom of individual leg movements were reduced by several constraints. First, the aluminum support where subject's foot was secured, sliding along the aluminum track, ensured standardized leg flexion and extensions. Additionally, the set-up was provided with a plastic rod which was used to stop the sliding of the foot support at an individual level of leg flexion accordingly with the execution of 1 s movement without moving the rest of the body. Second, participants had to perform a specific sequence of movements in a specific temporal window. This increased the level of uniformity of the performed footstep across subjects and, more importantly, across trials assuring that somatomotor inputs were as similar as possible between the repeated trials. Whereas, performing the footstep in the opposite direction, assured that somatomotor inputs (related to the footstep direction) were opposite between the non-repeated trails. Overall, all these constraints together with the intensive training and the instruction of performing a meaningful movement like a footstep are important factors that standardized the movement kinematics.

In all experiments, in order to minimize head movements a chin-neck rest was used during the scans. The chin-neck rest was constituted by a soft cervical collar, made of soft foam, supporting the subject's neck and chin. The cervical collar rested on the subjects' chest, greatly reducing head movements along the pitch axis (Pitzalis et al., 2019). The subjects' head was stabilized with foam padding, and additional foam pads were placed under their back and inion in order to reduce the level of discomfort. In all tasks, visual stimuli were presented on a monitor placed at the end of the scanner bore and viewed by participants via a mirror mounted on the head coil. In the integration experiment, visual motion stimulus (subtending 23° (H) x 13° (V) in visual angle) was generated by using a combination of MATLAB (The MathWorks Inc., Natick, MA, USA), Psychtoolbox-3 (Brainard, 1997; Pelli, 1997) and OpenGL.

2.5. Apparatus and procedure

Functional T2*-weighted images were collected using a gradient echo EPI sequence using blood-oxygenation level-dependent imaging (Kwong et al., 1992). Functional images were acquired using a 3T Philips Achieva MR scanner equipped for echo-planar imaging with a standard head coil and operating at the Neuroimaging Laboratory, Foundation Santa Lucia.

We used blood-oxygenation level-dependent imaging (Kwong et al., 1992) to acquire echo-planar functional MR images (TR = 2 s, TE=30 ms, flip angle=77°, 72 × 69 image matrix, 2.5 × 2.5 mm in-plane resolution, 38 slices, 3.6 mm slice thickness with 0.4 mm gap, ascending excitation order) in the AC–PC plane. Images were acquired starting from the superior convexity and extended ventrally so that to

include the whole cerebral cortex, except for the ventral portion of the cerebellum. For each participant we also acquired a three-dimensional high-resolution anatomical image using a turbo field echo sequence (TFE): TR= 13 ms, TE= 5.7 ms, flip angle=8°, 256 × 228 image matrix, 0.5 × 0.5 mm in-plane resolution, 342 contiguous 0.5 mm thick sagittal slices). For each scan, we discarded the first four volumes in order to achieve steady-state, and the experimental task was initiated at the beginning of the fifth volume.

We scanned participants during a single fMRI acquisition session including four 480-s long scans for the main experiment (also called "visuo-somatomotor integration experiment") and one anatomical scan. Each participant also completed two "localizer" experiments including two 256-s long flow field scans and one 526-s long leg movement scan. Data from these localizer scans were used to identify egomotion regions and somatomotor regions (see below).

2.6. Image processing and analysis

Images were preprocessed and analyzed using SPM12 (Wellcome Department of Cognitive Neurology, London, UK) and FreeSurfer 5.1 (http://surfer.nmr.mgh.harvard.edu/).

We first analyzed structural images following the "recon-all" fully automated processing pipeline implemented in FreeSurfer 5.1. This procedure allows us to obtain a surface representation of each individual cortical hemisphere in a standard space after performing intensity correction, transformation to Talairach space, normalization, skull-stripping, subcortical and white-matter segmentation, surface tessellation, surface refinement, surface inflation, sulcus-based nonlinear morphing to a cross-subject spherical coordinate system, and cortical parcellation (Dale et al., 1999; Fischl et al., 1999a,1999b; Desikan et al., 2006). The resulting surface reconstructions were transformed to the symmetrical FS-LR space (Van Essen et al., 2012) using tools in the Connectome Workbench software (https://www.humanconnectome.org/software/get-connectome-workbench), resulting in surface meshes with approximately 74 K nodes per hemisphere.

Functional images were realigned within and across scans to correct for head movement and coregistered with structural scans using SPM12 (Wellcome Department of Cognitive Neurology, London, UK). Functional data were then resampled to the individual cortical surface using ribbon-constrained resampling as implemented in Connectome Workbench (Glasser et al., 2013). Images were then spatially smoothed using a 6-mm full-width at half-maximum (FWHM) isotropic Gaussian kernel for the main experiment and a 4-mm FWHM isotropic Gaussian kernel for the localizer images. In order to reduce the impact of head movements on signal quality, the framewise displacement index (FD, Power et al., 2012) was quantified at each time point as an estimate in mm of head movement with respect to the previous time point and computed as the sum of the absolute values of the differentiated realignment estimates. FD values and six additional head movement-related regressors parameters (rotation and translation along the three axes x-y-z) were used as nuisance regressors in all the BOLD analyses. Additionally, to rule out any possible confounding effect induced by leg-movements over the head motion-related parameters, we analyzed FD as a function of the 2 by 2 (congruency by repetition) factorial design. This repeated-measures ANOVA revealed that there are no differences among factor levels. More specifically, we did not find either the congruency ($F_{1,29} = 1.140$; $p = 0.294$; $\eta_p^2 = 0.038$) or repetition main effects ($F_{1,29} = 0.239$; $p = 0.628$; $\eta_p^2 = 0.001$) or a significant congruency by repetition interaction ($F_{1,29} = 0.452$; $p = 0.507$; $\eta_p^2 = 0.015$). Thus, importantly for the interpretation of the BOLD results interpretation, head movement cannot explain the different activity profile observed between factor levels. Finally, to exclude any possible fatigue effect occurring during the experiment, we analyzed the FD values as a function of the experimental block (first, second, third, fourth). This one-way ANOVA revealed no significant block effect ($F_{1,29} = 1.619$; $p = 0.191$; $\eta_p^2 = 0.053$), thus indicating that no fatigue effect arising due to leg movements occurred during the experiment.

The conditions of our ethics approval do not permit public archiving of the raw MRI data. The preprocessed MRI anonymous data are available upon request at the lead author Pitzalis S. Access will be granted after completion of a formal data sharing agreement and approval of the local ethics committee, in accordance with ethical procedures governing the reuse of sensitive data. The experimental stimuli are available at the following link: https://github.com/valesulpizio/Multisensory-Integration-Experiment.

The analyses were conducted on two types of independently defined, theoretically motivated, regions of interest (ROIs): egomotion and somatomotor regions. These regions were identified by analyzing data from the "localizer" scans in which active blocks were modeled as box-car functions, convolved with a canonical hemodynamic response function.

Flow field scans were used to define three egomotion ROIs as the regions responding stronger to coherently versus randomly moving dots: (1) the posterior cingulate sulcus area (pCi), within the posterior dorsal tip of the cingulate sulcus. This region was originally labelled Pc (as Precuneus) by Cardin and Smith (2010), and later re-labelled pCi by Serra et al. (2019) to highlight its location within the cingulate sulcus; (2) the cingulate sulcus visual area (CSv), in the depth of the posterior part of the cingulate sulcus, anterior to the posterior ascending portion of the cingulate sulcus, corresponding to the original motion area described by Wall and Smith (2008); (3) the posterior insular cortex (PIC), at the junction between the posterior insula and the posterior parietal cortex (see Greenlee et al. 2016 for a review). Although the flow field stimulus activates six egomotion-related cortical regions (V6 +, V3A, VIP, pCi, CSv and PIC), only the three anterior ones, pCi, CSv, and PIC, have been studied in this work because they are also active during leg movements, thus indicating their possible role in the control of visually guided locomotion (Serra et al., 2019).

Leg movement scans were used to define three somatomotor ROIs as the regions responding stronger to leg movements relative to fixation: (1) the human homologue of the macaque area PEc (hPEc), recently defined in the anterior part of the dorsal precuneus (Pitzalis et al., 2019); (2) the medial portion of the human homologue of the macaque area PE (Pitzalis et al., 2019), right over the dorsal tip of the cingulate sulcus; (3) the medial portion of the primary somatosensory cortex (S-I) where the lower limb is represented (Di Russo et al., 2006; Akselrod et al., 2017; Tal et al., 2017).

The choice of defining egomotion (CSv, pCi, PIC) and somatomotor regions (hPEc, hPE, S-I) from separate contrasts of the two independent localizers was motivated by theoretical and technical reasons. Although functional ROIs can be created using orthogonal contrasts in a factorial design (Friston et al., 2006), as that used in our integration task, a common practice is to define the ROIs through a 'localizer' scan that is separate from the scan of primary interest, especially when an individually-based mapping is required (see Poldrack 2007; Saxe et al. 2006). Similarly, also a conjunction analysis between somatomotor and visual tasks could be potentially useful to identify all these regions. However, there are two important technical reasons why using these conjunction analyses would be unfeasible. First, the conjunction method is generally used to look for shared activation between two contrasts of the same task, rather than different contrasts of the separate tasks. Related to this point, it should be noted that the selected ROIs respond to somatomotor and visual tasks with very different intensities. Second, the watershed algorithm (see below) we applied here to segment the activation map and define ROIs around the individual activation peaks uses the intrinsic spatial gradient of the contrast map, which is partially disrupted by taking at each point the minimum of two maps as happens when using conjunction maps.

Both egomotion and somatomotor ROIs were created by using a threshold-free mapping, by selecting single activation peaks and their neighborhood (for a maximum of 400 cortical nodes) through a water-

Table 1
Regional peaks (MNI coordinates in mm) of somatomotor and egomotion ROIs.

Region	Hemisphere	MNI coordinates		
		X	Y	Z
hPEc	LH	−9 ± 5	−56 ± 5	64 ± 5
hPE	LH	−6 ± 2	−42 ± 3	68 ± 6
S-I	LH	−4 ± 4	−35 ± 4	69 ± 6
pCi	LH	−12 ± 3	−41 ± 4	49 ± 5
PIC	LH	−45 ± 5	−36 ± 5	19 ± 5
CSv	LH	−12 ± 2	−19 ± 4	40 ± 3

shed segmentation algorithm as applied to surface meshes (Mangan and Whitaker, 1999). This method ensures that all ROIs could be defined in every participant. All these ROIs were defined only in the left hemisphere to account for the fact that participants used their right leg during the main experiment. Table 1 reported MNI coordinates of regional peaks.

For the main experiment (*visuo-somatomotor integration* experiment) analysis, we modeled each trial as a canonical hemodynamic response function time-locked to the trial onset. We defined separate regressors for each experimental condition, by labeling each trial as a combination of Congruency (congruent, incongruent) and Repetition (repeated, non-repeated). The catch trials and the first trial following rest periods were modelled as separate conditions and were not considered in the analyses. For each participant and region, we computed a regional estimate of the amplitude of the hemodynamic response, by entering a weighted spatial average (across all vertices in the region) of the surface-transformed unsmoothed BOLD time series into the individual general linear models. Within each region, hemodynamic responses were analyzed with a 2 by 2 ANOVA, with Congruency between visual and somatomotor stimuli (congruent, incongruent) and Repetition (repeated, non-repeated) as main factors. For each of these analyses, post-hoc comparisons were computed after finding significant main effects and/or interactions, as paired T-tests with Bonferroni correction for multiple comparisons.

For this analysis, we used a Bonferroni adjustment in order to create confidence intervals for all the pairwise differences between the factor levels. This factorial design allowed us to explore integration properties of ROIs at two different hierarchical levels. As a first step, we verified whether a difference between congruent and incongruent bimodal conditions occurred at the level of the main factor Congruency. As a second step, we employed an fMR-adaptation paradigm in order to reveal, if any, more subtle differences in sensitivity to congruency relationship manipulation. Indeed, it has been argued that unimodal neurons might saturate the BOLD signal amplitude (ceiling effect), preventing response of bimodal neurons from emerging (Goebel and van Atteveldt, 2009). The fMR-adaptation paradigm was used to reduce the contribution of unimodal neurons to the BOLD signal amplitude, providing extra range where to test bimodal response. Assuming that a signal reduction observed in repeated trials compared to non-repeated trials reveals sensitivity to the repeated feature (fMR-adaptation), here we repeated bimodal congruent and incongruent pairs in order to reveal differential sensitivity to congruent and incongruent combinations. Indeed, a region which is sensitive to the congruency relationship between unimodal stimuli, adapting differently across congruent and incongruent conditions, should be involved in multisensory integration. Hence, the above-mentioned factorial design was also employed to verify, at the level of the main factor Repetition, whether ROIs showed lower responses to the Repeated condition compared to the Non-Repeated condition, revealing a general adaptation effect, *i.e.* a sensitivity to the repeated features (direction -right or left- of visual or somatomotor or either sensory modalities), regardless of their congruency relationship. Importantly, at the level of the interaction between the two main factors, a difference in adaptation effect across congruent and incongruent conditions would reveal a specific adaptation effect, *i.e.*, depending on Congruency. Finally, post-hoc analyses were used to confirm whether congruent- or an incongruent-specific adaptation had occurred and thus, whether a preference for congruent or incongruent cues exists, suggesting an involvement in multisensory integration.

Before submitting data to the above-mentioned parametric ANOVAs, the Kolmogorov–Smirnov test was applied to check for normality of the data distribution. The test indicated that variables were normally distributed ($p > 0.244$) in all regions, except in area hPE. In this area, we detected an asymmetric distribution ($p < 0.024$), induced by some outlier values. After delating these outlier values (2 subjects; z-score > 3), the Kolmogorov–Smirnov test have revealed that all variables were normally distributed ($p > 0.07$) so that parametric analyses (ANOVAs) were performed.

For completeness, we also conducted a whole-brain analysis. Parameter estimated images from each participant and condition entered a group analysis where subjects were treated as a random effect. An "omnibus" F-contrast comparing any combination of the two conditions (congruency and repetition) with the fixation condition was computed. The resulting statistical parametric map (shown in Supplementary Fig. S2) was thresholded at $p < 0.05$ FDR-corrected at the cluster level, with a cluster-forming threshold of $p < 0.001$ uncorrected.

3. Results

The histograms in Fig. 3A show the BOLD signal change as a function of Congruency (congruent vs. incongruent) and Repetition (repeated vs. non-repeated) in the somatomotor regions (hPEc, hPE and S-I) and in the egomotion regions (pCi, CSv and PIC). See also Supplementary Fig. S1 for a more detailed description about the distribution of individual data.

In order to assess whether all these regions were sensitive to the associative relationship between visual and somatomotor cues, we performed a neural adaptation analysis assessing whether repeated exposure to congruent/incongruent trials led to different adaptation effects. We thus analyzed the BOLD signal change as a function of Congruency (congruent vs. incongruent) and Repetition (repeated vs. non-repeated) by means of a 2 by 2 repeated-measure ANOVA.

Among the somatomotor regions, we found a main effect of Congruency only in hPEc ($F_{1,29} = 5.713$; $p = 0.024$; $\eta_p^2 = 0.165$), indicating a stronger response to incongruent as compared to congruent trials. No significant main effect of Congruency was observed in areas hPE ($F_{1,29} = 0.153$; $p = 0.698$; $\eta_p^2 = 0.005$) and S-I ($F_{1,29} = 0.021$; $p = 0.885$; $\eta_p^2 = 0.001$). The main effect of Repetition, which reflects the fMR-adaptation effect, *i.e.*, the reduction in neural activity following stimulus repetition (non-repeated > repeated), was found in all the somatomotor regions, *i.e.*, hPEc ($F_{1,29} = 5.655$; $p = 0.024$; $\eta_p^2 = 0.163$), hPE ($F_{1,27} = 4.699$; $p = 0.039$; $\eta_p^2 = 0.148$) and S-I ($F_{1,29} = 6.440$; $p = 0.017$; $\eta_p^2 = 0.182$). However, while the most anterior hPE and S-I showed a general sensitivity to the repeated presentation of bimodal stimuli, regardless of their spatial congruency, fMR-adaptation in area hPEc was also modulated by congruency. Indeed, the area showed a significant Congruency by Repetition interaction ($F_{1,29} = 5.080$; $p = 0.032$; $\eta_p^2 = 0.149$), indicating the presence of adaptation effects only for incongruent trials ($p = 0.005$). We found no significant interaction in areas hPE ($F_{1,29} = 0.061$; $p = 0.807$; $\eta_p^2 = 0.002$) and S-I ($F_{1,29} = 0.026$; $p = 0.873$; $\eta_p^2 = 0.001$).

Among the egomotion regions, we found a main effect of Congruency only in PIC ($F_{1,29} = 4.262$; $p = 0.048$; $\eta_p^2 = 0.128$), indicating a stronger response to congruent as compared to incongruent trials. No significant effect of Congruency was observed in areas CSv ($F_{1,29} = 0.717$; $p = 0.404$; $\eta_p^2 = 0.024$) and pCi ($F_{1,29} = 0.001$; $p = 0.985$; $\eta_p^2 = 0.001$). Repetition yielded significant fMR-adaptation in area CSv ($F_{1,29} = 10.366$; $p = 0.003$; $\eta_p^2 = 0.263$), but not in areas PIC ($F_{1,29} = 0.034$; $p = 0.856$; $\eta_p^2 = 0.001$) and pCi ($F_{1,29} = 2.408$; $p = 0.132$; $\eta_p^2 = 0.077$, indicating that only CSv was sensitive to the

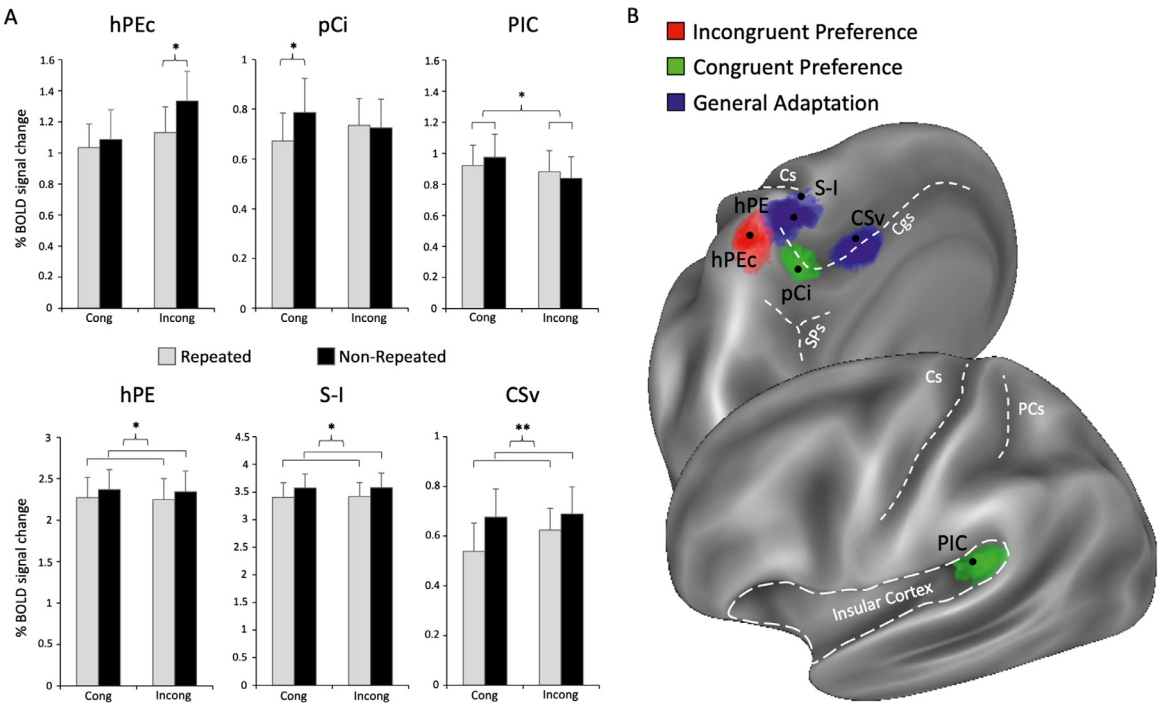

Fig. 3. ROIs sensitivity to the *visuo-somatomotor integration* experiment. (A) Column histograms plot the mean percentage of signal changes + SE of the mean across subjects in the tested regions. The upper part of the panel A shows regions which exhibited an integration effect (hPEc, pCi and PIC), while the lower part shows regions which did not exhibit an integration effect (hPE, S-I and CSv). ROIs responses are plotted as a function of Congruency (congruent vs. incongruent) and Repetition (repeated vs. non-repeated). Horizontal squared brackets denote averages between conditions. Horizontal curly brackets indicate statistical comparisons. Asterisks mark significant effects. * $p < 0.05$; ** $p < 0.005$. (B) Overlap of the six individually defined ROIs rendered on the inflated representation of the left hemisphere of Conte69 surface-based atlas. ROIs colors indicate in blue regions not showing integration effects (CSv, hPE and S-I), in green regions showing a congruent-specific integration effect (pCi and PIC) and in red the region (hPEc) showing an incongruent-specific integration effect. pCi: posterior cingulate sulcus area; CSv: cingulate visual area; PIC: posterior insular cortex; hPEc: human homologue of macaque area PEc; hPE: human homologue of macaque area PE; S-I: primary somatosensory cortex. (For interpretation of the references to color in this figure, the reader is referred to the web version of this article).

repeated exposure to identical trials. A significant Congruency by Repetition interaction was found only in pCi ($F_{1,29} = 4.690$; $p = 0.039$; $\eta_p^2 = 0.139$) and indicated the presence of adaptation effect only for congruent trials ($p = 0.027$). We found no significant interaction in area CSv ($F_{1,29} = 1.284$; $p = 0.266$; $\eta_p^2 = 0.042$) and a marginal significant interaction in area PIC ($F_{1,29} = 4.100$; $p = 0.052$; $\eta_p^2 = 0.124$).

In Fig. 3B each ROI is color-coded based on its response profile to the *visuo-somatomotor integration* experiment. To sum up, we found that somatomotor hPEc and egomotion regions pCi and PIC showed multisensory integration (Fig. 3A, upper panel), although in different ways. hPEc was the only region that showed a significant adaptation effect only for incongruent trials (red region in Fig. 3B). pCi and PIC showed a significantly increased response to the congruent combination of visual and somatomotor signals (green regions in Fig. 3B). In particular, pCi exhibited an fMR-adaptation effect only for congruent trials, while PIC responded stronger to congruent than incongruent trials. On the other side, somatomotor regions hPE and S-I, and egomotion area CSv did not show any evidence of integration between visual and somatomotor signals (Fig. 3A, lower panel). These regions indeed exhibited only fMR-adaptation effects, independently of the spatial congruency relationship between visual motion and leg movement (blue regions in Fig. 3B).

Finally, we also conducted a whole-brain analysis to corroborate the regional results. The "omnibus" F-contrast comparing any combination of the two conditions (Congruency and Repetition) with the fixation condition revealed that all the selected regions of interest are activated (see Supplementary Fig. S2).

4. Discussion

In the present work, we were interested in studying the integration properties of a set of multisensory regions (somatomotor regions hPEc, hPE, S-I and egomotion areas CSv, PIC, pCi), all showing both visual motion and somatomotor responses (Pitzalis et al., 2019; Serra et al., 2019; Di Marco et al., 2021). To this aim, we used an integration fMRI paradigm combining visual and somatomotor signals in a way that the direction of visual self-motion could be either compatible (congruent trials) or not (incongruent trials) with that of leg movements.

4.1. Multisensory integration in hPEc

The main finding in the present paper concerns the newly defined multisensory area hPEc. Here we found that this area is sensitive to the spatial congruency between visual and somatomotor stimuli suggesting that it is involved in multisensory integration processes. This result is new and significant in that it demonstrates what was previously only hypothesized first in macaque and then in humans.

Macaque PEc is indeed known to contain not only unimodal visual and unimodal somatosensory neurons, but also bimodal visuo-somatosensory neurons, and this led several authors to speculate that this region could be the ideal candidate for multisensory integration between the two sensory modalities (Breveglieri et al., 2006, 2008; Gamberini et al., 2018, 2020). However, differently from unimodal visual neurons (Battaglia-Mayer et al., 2001; Raffi et al., 2002, 2010, 2011, 2014), bimodal neurons have never been tested with an optic flow stimulus. Similarly, there are no monkey studies where the animal performs a limb movement while simultaneously receiving a visual stimulation to test the possible integrative properties of the bimodal neurons. Nevertheless, based on responses observed in this region to complex visual stimuli, particularly in the lower visual field, and a somatosensory representation of limbs, including the lower limbs, it has been suggested that PEc is involved in the control of locomotion (Breveglieri et al., 2006, 2008; Gamberini et al., 2018).

In humans, we have recently defined the human homologue of macaque PEc using a pure motor task and an innovative set-up for performing controlled leg movements. Like macaque PEc, we observed that hPEc is a multisensory region showing somatosensory, visuomotor, and visual properties. Indeed, this area responds to both arm and long-range leg movements, to both hand and foot pointing movements (Pitzalis et al., 2019) with a preference for the lower visual field (Maltempo et al., 2021), and to grasping movements (Sulpizio et al., 2020a), suggesting that this cortical region is involved in sensorimotor integration aimed at performing the action. In addition, we found that the sensorimotor hPEc is also implicated in processing egomotion-compatible visual motion, since it is sensitive to flow field (Pitzalis et al., 2019) and to self-motion compatible visual stimulation (Pitzalis et al., 2020). Additionally, in another recent study, we found that hPEc prefers a locomotion-compatible visual motion stimulus simulating changing direction of self-motion in the environment (*i.e.*, curved paths compared to linear paths), suggesting a role in encoding heading changes in the environment and path curvature, likely in order to estimate the future direction of self-motion and to control locomotor stability during steering (Di Marco et al., 2021). Based on this collective evidence, we originally speculated that hPEc is involved in the integration of visual and somatomotor cues, even though leg movements and optic flow were always tested separately (Pitzalis et al., 2019; Serra et al., 2019; Di Marco et al., 2021). Here, we substantiated this hypothesis by combining together visual and somatomotor cues in an integration fMRI experiment and showing for the first time that hPEc is implicated in multisensory integration of visual cues and somatomotor inputs coming from leg movements. Notably, here we found that area hPEc is able to differentiate between congruent and incongruent conditions (Fig. 3B, red-coded) since it adapted only for the incongruent condition. This suggests that hPEc is involved in signaling a mismatch between the multisensory signals with the aim of promoting adjustments of lower limb movements during locomotion and steering.

As mentioned above, macaque PEc contains bimodal visual-somatosensory neurons which have been suggested to be involved in controlling whole-body movements for interacting with the environment during visually-guided locomotion (Breveglieri et al., 2008). In these bimodal neurons, visual and somatosensory receptive are not spatially in register. Many bimodal neurons have a somatosensory receptive field near the shoulder and the visual receptive field distributed all over the visual field, in either central, peripheral, contralateral or ipsilateral visual space. Notice that while visual and somatosensory receptive fields in register could be useful in reaching and grasping an object, where the two types of information need to be coordinated, registered organization of visual and somatic information is less compelling for a more global interaction of the entire body with the flow of visual information coming from the entire visual environment during locomotion. As reminded above, in most bimodal cells of macaque PEc the somatosensory receptive field was located on the shoulder, which is presumably the joint most used by monkeys to control changing direction of movement during locomotion. Interestingly, due to upright position, humans use the hip to control changes in direction of movement as it happened in locomotion-compatible leg movements required in the present experiment. Notably, the activation of hPEc for concurrent hip stimulation and coherent visual motion we found here together with the preference for leg movements compared to arm movements (Pitzalis et al., 2019) supports the involvement of this region in controlling locomotion also in humans.

In some macaque regions, such as MSTd (Gu et al., 2006), VIP (Chen et al., 2011a) and VPS (Chen et al., 2011b), it has been described the presence of opposite neurons preferring opposite directions of self-motion (visual and vestibular cues). However, it is still unknown whether macaque PEc, among its bimodal neurons, hosts also opposite neurons (*i.e.*, cells preferring incongruent directions of visual and somatomotor cues to self-motion). Even if the functional role of opposite neurons is not clear, it has been hypothesized that these cells are responsible for discounting irrelevant visual motion information from the visual field (*e.g.*, Kim et al. 2016, Sasaki et al. 2017). It is possible that the preference for incongruent (opposite) cues in human PEc found here is underlain by such a mechanism, promoting a discounting of any kind of visual motion inputs (*e.g.*, locomotion irrelevant self-motion signals) which are incongruent with somatomotor inputs coming from leg movements during locomotion (see Billington and Smith 2015 for a similar interpretation).

The preference for incongruent cues found in hPEc is consistent with the involvement of the posterior parietal cortex (PPC) in the processing of incongruent stimuli. Indeed, in both macaques and humans PPC has been observed implicated in tasks where additional processing time was required for conflicting stimuli. For example, brain imaging human studies revealed an increased neural signal in the PPC following incongruent stimuli using a Stroop task (Adleman et al., 2002; Taylor et al., 1997; Carter et al., 1995; Bench et al., 1993). Also on macaque monkey, when PPC cells were tested using a task-switching task, it was found that the neuronal latencies to encode response related information were faster on congruent compared to incongruent trial (coherently with the longer behavioral reaction times associated with the incongruent stimuli; Stoet and Snyder, 2007). However, in these studies the mismatch condition is more related to a stimulus–response conflict, which needs to be resolved with a re-mapping of the motor response (*e.g.*, Pardo et al. 1990, Everling and Munoz 2000, Nakamura et al. 2005). Conversely, in the present study in the incongruent condition, conflicting stimuli were simultaneously presented and subjects did not have to re-map their motor response since this was based exclusively on an instruction (the visual cue indicating the leg movement direction) which was independent from the visual motion stimulation.

Overall, our result about the preference for incongruent cues found in hPEc provides evidence for the presence of opposite neurons in this region and demonstrates that hPEc is implicated in discounting irrelevant self-motion signals which are incongruent with somatomotor inputs arisen from leg movements for a stable perception of self-motion, likely promoting on-line adjustments of locomotion.

4.2. Multisensory integration in pCi and PIC

Another important result of this study is that we found positive evidence of multisensory integration in the cingulate and insular cortices in correspondence of the egomotion-related areas pCi and PIC. Unlike hPEc, areas pCi and PIC showed a congruent-specific integration effect (Fig. 3B, green-coded), with pCi exhibiting an adaptation effect only for congruent condition and PIC showing a preference for congruent as compared to incongruent condition. These findings suggest that pCi and PIC are involved in multisensory integration of visual and somatomotor cues to self-motion.

Since their discovery as motion areas, pCi and PIC were frequently associated to the egomotion network in that they respond to egomotion-compatible visual stimuli (Cardin and Smith, 2010, 2011; Huang et al., 2015; Pitzalis et al., 2020) and to flowfields (Serra et al., 2019; Sulpizio et al., 2020b). Area PIC is known as a multisensory region responding not only to visual (Frank et al., 2014, 2016a) but also to vestibular (Fasold et al., 2002; Smith et al., 2012) motion. Interestingly, macaque VPS (Chen et al., 2011b), which is thought to be the monkey counterpart of human PIC, contains bimodal neurons which are able to integrate visual and vestibular cues. These pieces of evidence led several authors to speculate that also in humans this region presumably supports the integration of visual and vestibular senses for the perception of self-motion (Frank et al., 2016a, 2016b). Thus, so far this region has only been tested for multisensory integration of visual and vestibular signals (Billington and Smith, 2015; Frank et al., 2014; 2016a, 2016b). Results showed that PIC is able to distinguish between congruent and incongruent combinations of visual cues and vestibular inputs coming from galvanic vestibular stimulation in MVPA analysis, although no differences had been observed in BOLD response (Billington and Smith, 2015).

Beside visual and vestibular properties, we have recently found evidence supporting the presence of motor response in both pCi and PIC. Indeed, in Serra et al. (2019) we found these regions were activated in a pure motor task where subjects were requested to perform long-range leg movements, suggesting a role of these regions in the motor control of lower limb movements.

In the present study, we proved that both pCi and PIC prefer congruent visual signals and somatomotor cues coming from leg movements suggesting that these areas are involved in multisensory integration. Present findings are in good agreement with previous literature. Indeed, the anterior portion of PIC and a region in proximity of the anatomical location of area pCi have been recently described as more activated by congruent as compared to incongruent combinations of visual and head motion signals, indicating a role in multimodal self-motion integration (Schindler and Bartels, 2018a).

All together, these findings indicate that pCi and PIC are able to integrate somatomotor inputs from both leg and head movements with congruent visual motion cues, likely being involved in controlling different body parts during self-motion. In particular, we suggest that these regions contain bimodal neurons integrating visual motion information and somatomotor signals from the lower limbs in order to guide heading changes during locomotion.

4.3. General adaptation in hPE, S-I and CSv

hPE, S-I and CSv did not show evidence for multisensory integration (Fig. 3B, blue-coded), but exhibited a general adaptation effect, indicating that these regions are sensitive to rightward and leftward direction of one (visual or somatomotor) or both sensory modalities (*i.e.*, the repeated unimodal feature in the bimodal stimulus). This general adaptation effect lends itself to various interpretations since all these three regions have visual as well as somatomotor responses.

PE and S-I are traditionally considered two low-level somatosensory regions and it is plausible that their human counterpart might be involved in encoding for rightward and leftward direction, at least in the somatomotor domain (*i.e.*, rightward and leftward rotation of the leg), rather than in high-level integration processes. However, note that some recent fMRI studies revealed that PE and S-I sensitivity can also be modulated by visual input (*e.g.*, Kuehn et al. 2018, Pitzalis et al. 2019, Di Marco et al. 2021, Maltempo et al. 2021). These findings have considerably challenged our understanding of the functions performed by the primary somatosensory cortices which would not only reflect processes of somatomotor stimuli but could actually be involved in the response to stimuli from other modalities. Importantly for the present paper, in Di Marco et al. (2021) we showed that both hPE and S-I prefer curve visual motion compared to linear visual motion, indicating their involvement in the analysis of visual motion related to changing direction of self-motion in the environment. These findings support the interpretation of the present results suggesting that hPE and S-I might be sensitive to rightward and leftward directions also in the visual domain (*i.e.*, rightward and leftward changing heading in forward visual motion). An alternative explanation is that heading changes during natural locomotion typically produce strong stimulation of leg joints (especially hip rotation) in order to turn the body. Thus, visual motion information provided during heading changes may be naturally associated with such a stimulation of leg joints so that the visual stimulation itself leads to a resonance effect evoking a pure somatomotor response in both hPE and S-I (see Di Marco et al. 2021 for similar data interpretation). Further studies are needed to verify these possibilities.

A similar reasoning can also be made for CSv, since it is an egomotion-related visual region showing high preference for coherent visual motion (Wall and Smith, 2008; Cardin and Smith, 2010; Serra et al., 2019; Pitzalis et al., 2020) and changes in direction of self-motion in the environment (Furlan et al., 2014; Di Marco et al., 2021), but it also exhibits vestibular (Smith et al., 2012) and somatomotor (Serra et al., 2019) responses. The absence of multisensory integration in CSv in our data is consistent with previous work (Billington and Smith, 2015) showing that this region does not exhibit differences between congruent and incongruent combinations of visual and vestibular cues either at the level of BOLD signal amplitude and by MVPA. In contrast, recent work studying multimodal integration between visual motion and signals provided by physical head movement in the scanner (Schindler and Bartels, 2018a) observed that CSv prefers congruent combinations compared to incongruent combinations, indicating that this region is able to integrate congruent signals. However, in line with the present results, it has been hypothesized that in CSv sensory signals about self-motion are merely collected to be separately sent to the motor system (with which this region is directly connected; Smith et al., 2018; Serra et al., 2019), rather than to be integrated (Smith et al., 2017). Indeed, the presence of multimodal sensory responses in a region does not necessarily imply that integration occurs (Huang and Sereno, 2018).

Overall, since in hPE, S-I and CSv we observed only a general adaptation effect, we can only speculate on the possible presence of an adaptation effect along the visual and/or the somatomotor dimension.

4.4. Functional considerations

The study of multisensory integration raises some methodological problems in both monkeys and humans. At the level of the single neuron, integration mechanisms have been extensively investigated in different multimodal domains. Multisensory integration can take different forms ranging from sub-additive to additive to super-additive effects (see Stein and Stanford 2008 for a review). Moreover, together with bimodal congruent neurons responding to multiple cues with congruent direction, also bimodal opposite neurons responding to multiple cues with incongruent direction were found (for a review see DeAngelis et al., 2012; see also Smith et al. 2017).

In humans, the issue of multisensory integration has been approached by employing different analysis strategies. In particular, recent fMRI studies have addressed this issue by comparing BOLD response between congruent and incongruent combinations of bimodal stimuli (Frank et al., 2014; Billington and Smith, 2015; Schindler and Bartels, 2018a, 2018b). Among them, two studies (Schindler and Bartels, 2018a, 2018b) found in some regions higher BOLD response for congruent combinations as compared to incongruent combinations, claiming that these areas integrate multimodal inputs. When univariate analysis failed to find a difference between congruent and incongruent conditions, some of these studies employed complementary multivariate pattern analysis (MVPA) (Billington and Smith, 2015; Schindler and Bartels, 2018b). Here, we opted for the fMRI-adaptation paradigm, which is considered more effective than standard fMRI approaches for studying multisensory integration, since it allows to reveal a difference in the adaptation effect between congruent and incongruent combinations which does not emerge at the level of the main effect of the congruency factor. Indeed, it has been argued that the limited dynamic range of BOLD amplitude might lead to saturation due to unimodal neuronal response, preventing bimodal neuronal response from emerging (Goebel and van Atteveldt, 2009). Also the MVPA allows to reveal in specific regions a difference between congruent and incongruent combinations. However, differently from MVPA, the fMRI-adaptation paradigm is informative about the direction of this difference, *i.e.*, which combination is preferred in a given region. This is an important point because, since neurons having either congruent or incongruent preferences have been observed in monkeys, we had no prior hypotheses about the sign of the difference between congruent and incongruent combinations. Indeed, by directly comparing adaptation effects between congruent and incongruent combinations, we revealed that among the three areas implicated in multisensory integration, one region exhibited a preference for congruent cues (pCi), whereas one region (hPEc) showed a preference for incongruent cues. Overall, the fMR-adaptation paradigm is confirmed as a successful strategy for studying multisensory integration processes (Goebel and van Atteveldt, 2009; van Atteveldt et al., 2010).

Lastly, a note on the type of leg movement the subjects were asked to perform here. As in our previous fMRI studies (Pitzalis et al., 2019; Serra et al., 2019; Di Marco et al., 2021), we used long-range leg movements in the scanner, but here for the first time subjects moved their leg simulating a footstep, with all the limits imposed by an fMRI study (for a behavioral study see Di Marco et al. 2019). Our paradigm was aimed at studying integration processes of coupled visual and somatomotor signals in a way as ecological as possible by providing a natural sequence of somatomotor inputs from the leg (as the ones we receive when we execute a footstep while walking), with particular importance of those evoked by the hip rotation which are specifically linked to heading changes during locomotion. Although to this aim, we used a modified version of the original set-up (Pitzalis et al., 2019; Serra et al., 2019; Di Marco et al., 2021) which ensures a wide and fluid rotation of every leg joint (see Methods for details), the movements were still executed only by one leg, an aspect that reduces the similarity to natural context. It should be noted that in a task as that used in the present study, we obviously expect similar effects also in the right hemisphere for left leg movements. However, future fMRI studies (with subjects moving both right and left limbs) are needed to determine whether the use of both legs might change the present results. We believe that even more intriguing would be using a completely different task, where the movements of the two legs are not only alternated but *coordinated* (like during real walking or cycling). We expect that a region, like hPEc (hosting neurons responding to both arm and leg; Breveglieri et al., 2008), would be much triggered by tasks like these, especially if also the subject's arms are engaged in performing the task. For the intrinsic difficulty in studying such a type of movement in the MR scanner, the few fMRI studies on this topic preferred presentation of videos showing human actions (*e.g.*, locomotion and climbing). For example, an interesting study by Abdollahi et al. (2013) revealed that the observation of climbing evoked activity in dorsal superior parietal lobule (SPL), in a region clearly including hPEc. Although we are aware of the scanner limitations, we acknowledge that future studies should investigate the neural bases of locomotion by using more ecologic setups requiring coordinated left and right leg movements which are closer to natural context.

5. Conclusions

In the present study, a differentiated response profile emerges among tested ROIs for multisensory integration of visual signals and somatomotor inputs from lower limbs associated with heading changes. While hPE, S-I and CSv do not show any integration effect but only a general adaptation effect, simply indicating a sensitivity to visual and/or somatomotor signals, PIC, pCi and hPEc, even if in different ways, show a multisensory integration effect. It is possible that hPEc, pCi and PIC are directly engaged in visually-guided locomotion control by sending visual and somatomotor signals to the motor system, likely in order to guide lower limb movements for steering actions during locomotion. Interestingly, hPEc shows a unique response profile with a preference for incongruent cues, suggesting that this region plays a pivotal role in more complex situations when mismatching inputs are present. It is possible that hPEc signals a mismatch between visual and somatomotor inputs, likely discounting visual signals which are incongruent with somatomotor inputs for a stable perception of self-motion and allowing the motor system for on-line adjustments during locomotion.

Declaration of Competing Interest

The authors declare that they have no known competing financial interests or personal relationships that could have appeared to influence the work reported in this paper.

Credit authorship contribution statement

Sara Di Marco: Conceptualization, Methodology, Software, Formal analysis, Investigation, Writing – original draft, Writing – review & editing. **Valentina Sulpizio:** Conceptualization, Methodology, Formal analysis, Writing – original draft, Writing – review & editing. **Martina Bellagamba:** Formal analysis, Investigation, Writing – review & editing. **Patrizia Fattori:** Writing – review & editing. **Gaspare Galati:** Methodology, Software, Writing – review & editing. **Claudio Galletti:** Conceptualization, Writing – review & editing. **Markus Lappe:** Writing – review & editing. **Teresa Maltempo:** Formal analysis, Investigation, Writing – review & editing. **Sabrina Pitzalis:** Conceptualization, Methodology, Supervision, Project administration, Writing – original draft, Writing – review & editing.

Acknowledgments

The work was supported by the University of Rome "Foro Italico", Italy, grant to Sabrina Pitzalis (CDR2.FFABR), and by the University of Bologna (MIUR-PRIN 2017 KZNZLN). We thank F. Di Russo for helping with the set-up construction and F. Strappini for helping with Fig. 1.

Data and code availability statement

We stated the following sentence in the manuscript methods section.

"The conditions of our ethics approval do not permit public archiving of the raw MRI data. The preprocessed MRI anonymous data are available upon request at the lead author Pitzalis S. Access will be granted after completion of a formal data sharing agreement and approval of the local ethics committee, in accordance with ethical procedures governing the reuse of sensitive data. The experimental stimuli are available at the following link: https://github.com/valesulpizio/Multisensory-Integration-Experiment."

Supplementary materials

Supplementary material associated with this article can be found, in the online version, at doi:10.1016/j.neuroimage.2021.118581.

References

Abdollahi, R.O., Jastorff, J., Orban, G.A., 2013. Common and segregated processing of observed actions in human SPL. Cereb. Cortex 23, 2734–2753.
Adleman, N.E., Menon, V., Blasey, C.M., White, C.D., Warsofsky, I.S., Glover, G.H., et al., 2002. A developmental fMRI study of the stroop color–word task. Neuroimage 16, 61–75.
Akselrod, M., Martuzzi, R., Serino, A., van der Zwaag, W., Gassert, R., Blanke, O., 2017. Anatomical and functional properties of the foot and leg representation in areas 3b, 1 and 2 of primary somatosensory cortex in humans: a 7 T fMRI study. Neuroimage doi:10.1016/j.neuroimage.2017.06.021.
Bakola, S., Gamberini, M., Passarelli, L., Fattori, P., Galletti, C., 2010. Cortical connections of parietal field PEc in the macaque: linking vision and somatic sensation for the control of limb action. Cereb. Cortex 20, 2592–2604. doi:10.1093/cercor/bhq007.
Battaglia-Mayer, A., Ferraina, S., Genovesio, A., Marconi, B., Squatrito, S., Molinari, M., Lacquaniti, F., Caminiti, R., 2001. Eye-hand coordination during reaching. II. An analysis of the relationships between visuomanual signals in parietal cortex and parieto-frontal association projections. Cereb. Cortex 11, 528–544.
Bench, C.J., Frith, C.D., Grasby, P.M., Friston, K.J., Paulesu, E., Frackowiak, R.S., et al., 1993. Investigations of the functional anatomy of attention using the Stroop test. Neuropsychologia 31, 907–922.
Billington, J., Smith, A.T., 2015. Neural Mechanisms for discounting head-roll-induced retinal motion. J. Neurosci. 35 (12), 4851–4856. doi:10.1523/JNEUROSCI.3640-14.2015.
Brainard, D.H., 1997. The psychophysics toolbox. Spat. Vis. 10, 433–436.
Bremmer, F., Kubischik, M., Pekel, M., Lappe, M., Hoffmann, K.P., 1999. Linear vestibular self-motion signals in monkey medial superior temporal area. Ann. N.Y. Acad. Sci. 871, 272–281.
Breveglieri, R., Galletti, C., Gamberini, M., Passarelli, L., Patrizia, F., 2006. Somatosensory cells in area PEc of macaque posterior parietal cortex. J. Neurosci. 26, 3679–3684.
Breveglieri, R., Galletti, C., Monaco, S., Fattori, P., 2008. Visual, somatosensory, and bimodal activities in the macaque parietal area PEc. Cereb. Cortex 18, 806–816.
Cardin, V., Smith, A.T., 2010. Sensitivity of human visual and vestibular cortical regions to egomotion-compatible visual stimulation. Cereb. Cortex 20, 1964–1973. doi:10.1093/cercor/bhp268.
Cardin, V., Smith, A.T., 2011. Sensitivity of human visual cortical area V6 to stereoscopic depth gradients associated with self-motion. J. Neurophysiol. 106, 1240–1249. doi:10.1152/jn.01120.2010.
Carter, C.S., Mintun, M., Cohen, J.D., 1995. Interference and facilitation effects during selective attention: an H2 15O PET study of Stroop task performance. Neuroimage 2, 264–272.

Chen, A., DeAngelis, G.C., Angelaki, D.E., 2013. Functional specializations of the ventral intraparietal area for multisensory heading discrimination. J. Neurosci. 33, 3567.
Chen, A., DeAngelis, G.C., Angelaki, D.E., 2011a. Representation of vestibular and visual cues to self-motion in ventral intraparietal cortex. J. Neurosci. 31, 12036–12052.
Chen, A., DeAngelis, G.C., Angelaki, D.E., 2011b. Convergence of vestibular and visual self-motion signals in an area of the posterior sylvian fissure. J. Neurosci. Off. J. Soc. Neurosci., 31 (32), 11617–11627. doi:10.1523/JNEUROSCI.1266-11.2011.
Christensen, M.S., Lundbye-Jensen, J., Petersen, N., Geertsen, S.S., Paulson, O.B., Nielsen, J.B., 2007. Watching your foot move – an fMRI study of visuomotor interactions during foot movement. Cereb. Cortex 17 (8), 1906–1917. doi:10.1093/cercor/bhl101.
Crowell, J. A., Banks, M. S., 1993. Perceiving heading with different retinal regions and types of optic flow. Perception & Psychophysics 53, 325–337.
Cutting, J. E., Vishton, P. M., Fluckiger, M., Baumberger, B., Gerndt, J. D., 1997. Heading and path information from retinal flow in naturalistic environments. Perception & Psychophysics 59, 426–441.
Dale, A.M., Fischl, B., Sereno, M.I., 1999. Cortical surface-based analysis I Segmentation and surface reconstruction. Neuroimage 9, 179–194.
Dalla Volta, R., Fasano, F., Cerasa, A., Mangone, G., Quattrone, A., Buccino, G, 2015. Walking indoors, walking outdoors: an fMRI study. Front. Psychol. 6, 1–10. doi:10.3389/fpsyg.2015.01502.
DeAngelis, G.C., Angelaki, D.E., Murray, M.M., Wallace, M.T., 2012. The neural bases of multisensory processes frontiers. Neuroscience.
Desikan, R.S., Ségonne, F., Fischl, B., Quinn, B.T., Dickerson, B.C., Blacker, D., Buckner, R.L., Dale, A.M., Maguire, R.P., Hyman, B.T., 2006. An automated labeling system for subdividing the human cerebral cortex on MRI scans into gyral based regions of interest. Neuroimage 31, 968–980.
Di Marco, S., Tosoni, A., Altomare, E.C., Ferretti, G., Perrucci, M.G., Committeri, G., 2019. Walking-related locomotion is facilitated by the perception of distant targets in the extrapersonal space. Sci. Rep. 9, 9884. doi:10.1038/s41598-019-46384-5.
Di Marco, S., Fattori, P., Galati, G., Galletti, C., Lappe, M., Maltempo, T., Serra, C., Sulpizio, V., Pitzalis, S., 2021. Preference for locomotion-compatible path curvature from the optic flow in leg-related somatomotor regions and egomotion-related visual areas. Cortex 137, 74–92. doi:10.1016/j.cortex.2020.12.021.
Di Russo, F., Committeri, G., Pitzalis, S., Spitoni, G., Piccardi, L., Galati, G., Catagni, M., Nico, D., Guariglia, C., Pizzamiglio, L., 2006. Cortical plasticity following surgical extension of lower limbs. Neuroimage 30, 172–183. doi:10.1016/j.neuroimage.2005.09.051.
Duffy, C. J., 1998. MST neurons respond to optic flow and translational movement. J. Neurophysiol. 80, 1816–1827. doi:10.1152/jn.1998.80.4.1816.
Everling, S., Munoz, D.P., 2000. Neuronal correlates for preparatory set associated with pro-saccades and anti-saccades in the primate frontal eye field. J. Neurosci. 20, 387–400.
Fasold, O., von Brevern, M., Kuhberg, M., Ploner, C.J., Villringer, A., Lempert, T., Wenzel, R., 2002. Human vestibular cortex as identified with caloric stimulation in functional magnetic resonance imaging. Neuroimage 17 (3), 1384–1393. doi:10.1006/nimg.2002.1241.
Fischl, B., Sereno, M.I., Dale, A.M., 1999a. Cortical surface-based analysis: II. Inflation, flattening, and a surface-based coordinate system. Neuroimage 9 (2), 195–207. doi:10.1006/nimg.1998.0396.
Fischl, B., Sereno, M.I., Tootell, R.B.H., Dale, A.M., 1999b. High-resolution intersubject averaging and a coordinate system for the cortical surface. Hum Brain Mapp 8, 272–284. doi:10.1002/(SICI)1097-0193(1999)8:4<272-AID-HBM10>3.0.CO;2-4.
Frank, S.M., Baumann, O., Mattingley, J.B., Greenlee, M.W., 2014. Vestibular and visual responses in human posterior insular cortex. J. Neurophysiol. 112, 2481–2491.
Frank, S.M., Wirth, A.M., Greenlee, M.W., 2016a. Visual-vestibular processing in the human Sylvian fissure. J. Neurophysiol. 116, 263–271. doi:10.1152/jn.00009.2016.
Frank, S.M., Sun, L., Forster, L., Peter, U.T., Greenlee, M.W., 2016b. Cross-modal attention effects in vestibular cortex during attentive tracking of moving objects. The Journal of Neuroscience 36 (50), 12720–12728. doi:10.1523/JNEUROSCI.2480-16.2016.
Friston, K.J., Rotshtein, P., Geng, J.J., Sterzer, P., Henson, R.N., 2006. A critique of functional localisers. Neuroimage 30, 1077–1087.
Furlan, M., Wann, J.P., Smith, A.T., 2014. A representation of changing heading direction in human cortical areas pVIP and CSv. Cereb. Cortex 24 (11), 2848–2858. doi:10.1093/cercor/bht132.
Gamberini, M., Dal Bò, G., Breveglieri, R., Briganti, S., Passarelli, L., Fattori, P., Galletti, C., 2018. Sensory properties of the caudal aspect of the macaque's superior parietal lobule. Brain Struct. Funct. 223, 1863–1879.
Gamberini, M., Passarelli, L., Fattori, P., Galletti, C., 2020. Structural connectivity and functional properties of the macaque superior parietal lobule. Brain Struct. Funct. 225, 1349–1367. doi:10.1007/s00429-019-01976-9.
Glasser, M.F., Sotiropoulos, S.N., Wilson, J.A., Coalson, T.S., Fischl, B., Andersson, J.L., Xu, J., Jbabdi, S., Webster, M., Polimeni, J.R., Van Essen, D.C., Jenkinson, M., 2013. The minimal preprocessing pipelines for the human connectome project. Neuroimage 80, 105–124.
Goebel, R., van Atteveldt, N., 2009. Exp. Brain. Res. 198, 153. doi:10.1007/s00221-009-1881-7.
Greenlee, M.W., Frank, S.M., Kaliuzhna, M., Blanke, O., Bremmer, F., Churan, J., Cuturi, L.F., MacNeilage, P.R., Smith, A.T., 2016. Multisensory integration in self motion perception. Multisens. Res. 29 (6–7), 525–556. doi:10.1163/22134808-00002527.
Gu, Y., Angelaki, D.E., DeAngelis, G.C., 2008. Neural correlates of multisensory cue integration in macaque MSTd. Nat. Neurosci. 11, 1201–1210.
Gu, Y., Watkins, P.V., Angelaki, D.E., DeAngelis, G.C., 2006. Visual and nonvisual contributions to three-dimensional heading selectivity in the medial superior temporal area. J Neurosci 26, 73–85.
Heed, T., Beurze, S.M., Toni, I., Röder, B., Medendorp, W.P., 2011. Functional rather than effector-specific organization of human posterior parietal cortex. J. Neurosci. 31, 3066–3076.
Heed, T., Leone, F.T.M., Toni, I., Medendorp, W.P., 2016. Functional versus effector- specific organization of the human posterior parietal cortex: revisited. J. Neurophysiol. 116, 1885–1899.
Huang, R.S., Chen, C., Tran, A.T., Holstein, K.L., Sereno, M.I., 2012. Mapping multisensory parietal face and body areas in humans. Proc. Natl. Acad. Sci. U. S. A., 109, 18114–18119.
Huang, R.S., Chen, C.F., Sereno, M.I., 2015. Neural substrates underlying the passive observation and active control of translational egomotion. J. Neurosci. 35 (10), 4258–4267. doi:10.1523/JNEUROSCI.2647-14.2015.
Huang, R., Sereno, M.I., 2018. Multisensory and sensorimotor maps, 1st ed. The Parietal Lobe. Elsevier B.V.
Kapreli, E., Athanasopoulos, S., Papathanasiou, M., Van Hecke, P., Kelekis, D., Peeters, R., Sunaert, S., 2008. Lower limb sensorimotor network: issues of somatotopy and overlap. Cortex 43 (2), 219–232. doi:10.1016/S0010-9452(08)70477-5.
Kim, H.R., Pitkow, X., Angelaki, D.E., DeAngelis, G.C., 2016. A simple approach to ignoring irrelevant variables by population decoding based on multisensory neurons. J. Neurophysiol. 116:1449–1467. doi:10.1152/jn.00005.2016
Kuehn, E., Haggard, P., Villringer, A., Pleger, B., Sereno, M.I., 2018. Visually-driven maps in Area 3b. J. Neurosci. 38 (5), 1295–1310. doi:10.1523/JNEUROSCI.0491-17.2017, Jan 31Epub 2018 Jan 4.
Kwong, K.K., Belliveau, J.W., Chesler, D.A., Goldberg, I.E., Weisskoff, R.M., Poncelet, B.P., Kennedy, D.N., Hoppel, B.E., Cohen, M.S., Turner, R., 1992. Dynamic magnetic resonance imaging of human brain activity during primary sensory stimulation. Proc. Natl. Acad. Sci. U. S. A. 89, 5675–5679. doi:10.1073/pnas.89.12.5675.
Leone, F.T.M., Heed, T., Toni, I., Medendorp, W.P., 2014. Understanding effector selectivity in human posterior parietal cortex by combining information patterns and activation measures. J. Neurosci. 34, 7102–7112.
Li, L., Cheng, J.C., 2011. Perceiving path from optic flow. J. Vis. 11 (1), 22. doi:10.1167/11.1.22, Jan 26pii.
Lorey, B., Naumann, T., Pilgramm, S., Petermann, C., Bischoff, M., Zentgraf, K., … Munzert, J., 2014. How equivalent are the action execution, imagery, and observation of intransitive movements? revisiting the concept of somatotopy during action simulation. Brain Cogn. 81 (1), 139–150. doi:10.1016/j.bandc.2012.09.011.
Maltempo, T., Pitzalis, S., Bellagamba, M., Di Marco, S., Fattori, P., Galati, G., Galletti, C., Sulpizio, V., 2021. Lower visual field preference for the visuomotor control of limb movements in the human dorsomedial parietal cortex. Brain Struct. Funct. doi:10.1007/s00429-021-02254-3.
Mangan, A.P., Whitaker, R.T., 1999. Partitioning 3D surface meshes using watershed segmentation. IEEE Trans. Vis. Comput. Graph. 5 (4), 308–321.
Nakamura, K., Roesch, M.R., Olson, C.R., 2005. Neuronal activity in macaque SEF and ACC during performance of tasks involving conflict. J. Neurophysiol. 93, 884–908.
Oldfield, R.C., 1971. The assessment and analysis of handedness: the Edinburgh inventory. Neuropsychologia 9, 97–113. doi:10.1016/0028-3932(71)90067-4.
Pardo, J.V., Pardo, P.J., Janer, K.W., Raichle, M.E., 1990. The anterior cingulate cortex mediates processing selection in the Stroop attentional conflict paradigm. Proc. Natl. Acad. Sci. U.S.A., 87, 256–259.
Pelli, D.G., 1997. The VideoToolbox software for visual psychophysics: transforming numbers into movies. Spat. Vis. 10 (4), 437–442 1997.
Pitzalis, S., Sereno, M.I., Committeri, G., Fattori, P., Galati, G., Patria, F., Galletti, C., 2010. Human V6: the medial motion area. Cereb. Cortex 20, 411–424.
Pitzalis, S., Serra, C., Sulpizio, V., Di Marco, S., Fattori, P., Galati, G., Galletti, C., 2019. A putative human homologue of the macaque area PEc. Neuroimage doi:10.1016/j.neuroimage.2019.116092, In press.
Pitzalis, S., Serra, C., Sulpizio, V., Committeri, G., de Pasquale, F., Fattori, P., Galletti, C., Sepe, R., Galati, G., 2020. Neural bases of self- and object-motion in a naturalistic vision. Hum. Brain Mapp. doi:10.1002/hbm.24862, Nov 11.
Poldrack, R.A., 2007. Region of interest analysis for fMRI. Soc. Cogn. Affect. Neurosci. 2, 67–70. doi:10.1093/scan/nsm006.
Power, J.D., Barnes, K.A., Snyder, A.Z., Schlaggar, B.L., Petersen, S.E., 2012. Spurious but systematic correlations in functional connectivity MRI networks arise from subject motion. Neuroimage 59 (3), 2142–2154. doi:10.1016/j.neuroimage.2011.10.018.
Raffi, M., Carrozzini, C., Maioli, M.G., Squatrito, S., 2010. Multimodal representation of optic flow in area PEc of macaque monkey. Neuroscience 171, 1241–1255. doi:10.1016/j.neuroscience.2010.09.026.
Raffi, M., Maioli, M.G., Squatrito, S., 2011. Optic flow direction coding in area PEc of the behaving monkey. Neuroscience 194, 136–149. doi:10.1016/j.neuroscience.2011.07.036.
Raffi, M., Persiani, M., Piras, A., Squatrito, S., 2014. Optic flow neurons in area PEc integrate eye and head position signals. Neurosci. Lett. 568, 23–28. doi:10.1016/j.neulet.2014.03.042.
Raffi, M., Squatrito, S., Maioli, M.G., 2002. Neuronal responses to optic flow in the monkey parietal area PEc. Cereb.Cortex 12, 639–646.
Rocca, M.A., Filippi, M., 2010. FMRI correlates of execution and observation of foot movements in left-handers. J. Neurol. Sci. 288 (1–2), 34–41. doi:10.1016/j.jns.2009.10.013.
Sacheli, L.M., Zapparoli, L., De Santis, C., et al., 2017. Mental steps: differential activation of internal pacemakers in motor imagery and in mental imitation of gait. Hum. Brain Mapp. 38, 5195–5216.
Sahyoun, C., Floyer-Lea, A., Johansen-Berg, H., Matthews, P.M., 2004. Towards an understanding of gait control: brain activation during the anticipation, preparation and execution of foot movements. Neuroimage 21 (2), 568–575. doi:10.1016/j.neuroimage.2003.09.065.

Sasaki, R., Angelaki, D.E., DeAngelis, G.C., 2017. Dissociation of self-motion and object motion by linear population decoding that approximates marginalization. The Journal of Neuroscience 37, 11204–11219. doi:10.1523/JNEUROSCI.1177-17.2017.

Saxe, R., Brett, M., Kanwisher, N., 2006. Divide and conquer: a defense of functional localizers. Neuroimage 30, 1088–1096.

Schindler, A., Bartels, A., 2018a. Integration of visual and non-visual self-motion cues during voluntary head movements in the human brain. Neuroimage 172, 597–607. doi:10.1016/j.neuroimage.2018.02.006.

Schindler, A., Bartels, A., 2018b. Human V6 integrates visual and extra-retinal cues during head-induced gaze shifts. iScience 7, 191–197. doi:10.1016/j.isci.2018.09.004.

Schlack, A., Hoffmann, K.P., Bremmer, F., 2002. Interaction of linear vestibular and visual stimulation in the macaque ventral intraparietal area (VIP). Eur. J. Neurosci 16, 1877–1886. doi:10.1046/j.1460-9568.2002.02251.x.

Serra, C., Galletti, C., Di Marco, S., Fattori, P., Galati, G., Sulpizio, V., Pitzalis, S., 2019. Egomotion-related visual areas respond to active leg movements. Hum. Brain. Mapp. 40, 3174–3191. doi:10.1002/hbm.24589.

Smith, A.T., Greenlee, M.W., DeAngelis, G.C., Angelaki, D.E., 2017. Distributed visual–vestibular processing in the cerebral of man and macaque. Multisens. Res. 30, 91–120.

Smith, A.T., Beer, A.L., Furlan, M., Mars, R.B., 2018. Connectivity of the cingulate sulcus visual area (CSv) in the human cerebral cortex. Cereb. Cortex 28 (2), 713–772. doi:10.1093/cercor/bhx002.

Smith, A.T., Wall, M.B., Thilo, K.V., 2012. Vestibular inputs to human motion-sensitive visual cortex. Cereb. Cortex 22, 1068–1077. doi:10.1093/cercor/bhr179.

Sood, M.R., Sereno, M.I., 2016. Areas activated during naturalistic reading comprehension overlap topological visual, auditory, and somatotomotor maps. Hum. Brain Mapp. 37, 2784–2810.

Stein, B.E., Stanford, T.R., 2008. Multisensory integration: current issues from the perspective of the single neuron. Nat. Rev. Neurosci. 9, 255–266.

Stoet, G., Snyder, L.H., 2007. Correlates of stimulus–response congruence in the posterior parietal cortex. J. Cogn. Neurosci. 19 (2), 194–203.

Sulpizio, V., Neri, A., Fattori, P., Galletti, C., Pitzalis, S., Galati, G., 2020a. Real and imagined grasping movements differently activate the human dorsomedial parietal cortex. Neuroscience 434, 22–34.

Sulpizio, V., Galati, G., Fattori, P., Galletti, C., Pitzalis, S., 2020b. A common neural substrate for processing scenes and egomotion-compatible visual motion. Brain Struct. Funct.

Tal, Z., Geva, R., Amedi, A., 2017. Positive and negative somatotopic bold responses in contralateral versus ipsilateral penfield homunculus. Cereb. Cortex doi:10.1093/cercor/bhx024.

Taylor, S.F., Kornblum, S., Lauber, E.J., Minoshima, S., Koeppe, R.A., 1997. Isolation of specific interference processing in the Stroop task: PET activation studies. Neuroimage 6, 81–92.

van Atteveldt, N.M., Blau, V.C., Blomert, L., et al., 2010. fMR-adaptation indicates selectivity to audiovisual content congruency in distributed clusters in human superior temporal cortex. BMC Neurosci. 11, 11. doi:10.1186/1471-2202-11-11.

Van Essen, D.C., Glasser, M.F., Dierker, D.L., Harwell, J., Coalson, T., 2012. Parcellations and hemispheric asymmetries of human cerebral cortex analyzed on surface-based atlases. Cereb. Cortex 22, 2241–2262. doi:10.1093/cercor/bhr291.

Wall, M.B., Smith, A.T., 2008. The representation of egomotion in the human brain. Curr. Biol. 18, 191–194. doi:10.1016/j.cub.2007.12.053.